He Liu*, Jianguo Jiang Wei Luo

J. Electrical Systems 11-3 (2015): 271-280

Regular paper

A Comparative Analysis of the Three-Level NPC and ANPC Converter Loss Distribution

In this paper, a comparative analysis of the three-level NPC and ANPC converter loss distribution are presented. Switching states and commutation principle of two topologies are analyzed and compared; Also, the loss distribution mathematical model of the two topologies has been established. The main feature of the three-level ANPC structure is to use the switching devices to replace the clamp diodes of the three-level NPC topology, by selecting the different zero voltage state. As a result, it can realize the loss distribution balance among the power devices. Then, the simulation results are shown the effectiveness of the three-level ANPC topology as it can realize the power devices loss equalize under different work conditions, and verified the validity of the proposed loss distribution mathematical model.

Keywords: multilevel converters; three-level ANPC converter; loss distribution.

1. Introduction

Three-level neutral point clamped (3L-NPC) converter has been widely used in high-power medium-voltage applications since it was proposed in 1980[1].The main drawback of 3L-NPC is the loss distribution imbalance among the power devices [2]-[4]. Three-level ANPC (3L-ANPC) topology is an effective method to solve this problem, by using switching devices to replace the 3L-NPC clamp diodes. As a result, it can change the loss distribution of the power devices by switching different zero states in the commutation strategy [5]-[7]. In this dissertation, the commutation path and the loss distribution models of two topologies have been analyzed. Then, the simulation results are presented to validate the theoretical studies as three-level ANPC topology can realize the loss equalize of the power devices.

2. Notation

The notation used throughout the paper is stated below.

Indexes:

V_{dc}	DC-link voltage (V)
φ	power factor of the inverter
S_{ax}	switch *x* of the bridge arm *a*
D_{ax}	diode *x* of the bridge arm *a*
p_{inv}	total loss of the inverter (W)
$p_{conduct\text{-}half}$	conduction loss of the inverter in half modulation cycle (W)
$p_{sw\text{-}half}$	switching loss of the inverter in half modulation cycle (W)
$p_{conduct\text{-}S}$	conduction loss of all the switches in half modulation cycle(W)

* Corresponding author: He Liu, Key Laboratory of Control of Power Transmission and Conversion, Ministry of Education (Department of Electrical Engineering, Shanghai Jiao Tong University), Shanghai 200030, China, E-mail: elec_studio@sjtu.edu.cn

$p_{conduct-D}$	conduction loss of all the diodes in half modulation cycle(W)
p_{sw-Sax}	switching loss of switch *x* in bridge arm *a* (W)
$p_{rec-Dax}$	reverse recovery loss of diode *x* in bridge arm *a*(W)
$p_{conduct-Sax}$	conduction loss of switch *x* in bridge arm *a*(W)
$p_{conduct-Dax}$	conduction loss of diode *x* in bridge arm *a*(W)
k_{φ}	number of pulses of the phase voltage before phase current crossing zero
m_{f}	carry wave radio of the inverter
d_{k}	when the *k-th* pulse, pulse duty of switch *x*
v_{onSax_k}	when the *k-th* pulse, the conduction voltage drop of switch S_{ax}
v_{onDax_k}	when the *k-th* pulse, the conduction voltage drop of diode D_{ax}
E_{swSax_k}	when the *k-th* pulse, the switching loss of switch S_{ax}
E_{recDax_k}	when the *k-th* pulse, the reverse recovery loss of diode D_{ax}
T	period of the phase voltage
f	frequency of the phase voltage , $f = 1 / T$

Constants:

T_s	period of the carry wave
f_s	frequency of the carry wave , $f_s = 1/T_s$
r_T	conduction resistance of the switching device
v_{T0}	conduction loss of the switching device in normal working conduction

3. Three level NPC operating principle and power loss distribution

The topology of 3L-NPC convert is shown in Figure 1, Table 1 summarizes its switching states.

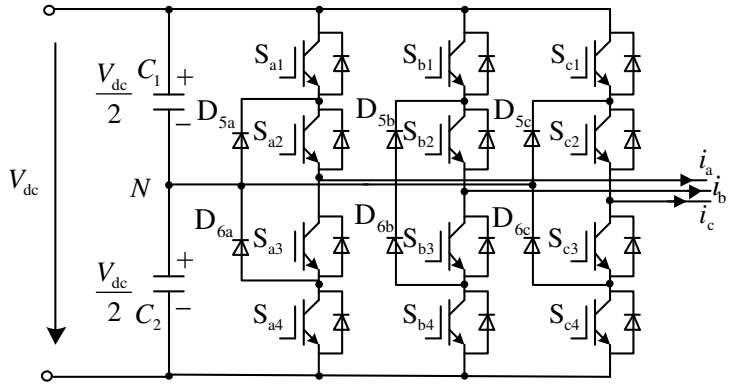

Fig.1. Three-level NPC converter.

Phase A is chosen as an illustrative example, when the switch state is state P as the switch S_{a1}, S_{a2} are turned on. The clamping diode D_{5a} makes the switch S_{a1}, S_{a2} withstand the negative arm capacitor voltage. When the inverter output voltage state is state O, the middle switches of the converter S_{a2} , S_{a3} are turned on. When the current direction is positive as shown in Fig.1, phase A is connected to the neutral point through D_{5a} and S_{a2} .

Table 1. Phase A switch sequence of three level NPC inverter

Output voltage v_{aN}	Switch States	S_{a1}	S_{a2}	S_{a3}	S_{a4}
V_{dc} / 2	P	1	1	0	0
0	O	0	1	1	0
$-V_{dc}$ / 2	N	0	0	1	1

Due to the symmetry of the three-phase output voltage, take the phase A as an example to analyze the loss distribution characteristics of 3L-NPC converter. Assuming the converter output power factor angle is φ, Table 2 summarizes the switching state changes and loss distribution characteristics of 3L-NPC converter in one voltage command cycle.

Table 2. Phase A switch-state of three level NPC converter in a cycle.

Conduct angle	Switch state	Phase voltage	Load current	Switching device
0-φ	P/O	V_{dc} / 2、-V_{dc} / 2	Negative	D_{a1}、D_{a2} S_{a3}、D_{6a}
φ-π	P/O	V_{dc} / 2、-V_{dc} / 2	Positive	S_{a1}、S_{a2} D_{5a}、S_{a2}
(π+φ)-2π	O/N	0、-V_{dc} / 2	Negative	D_{5a}、S_{a2}
π □ (2π-φ)	O/N	0、-V_{dc} / 2	Positive	D_{6a}、S_{a3} S_{a3}、S_{a4}

Note : D_{ax} in Table 2 represent the parasitic diode of the IGBT

Figure 2 is a schematic view of the drive pulses and the load current of 3L-NPC convert.

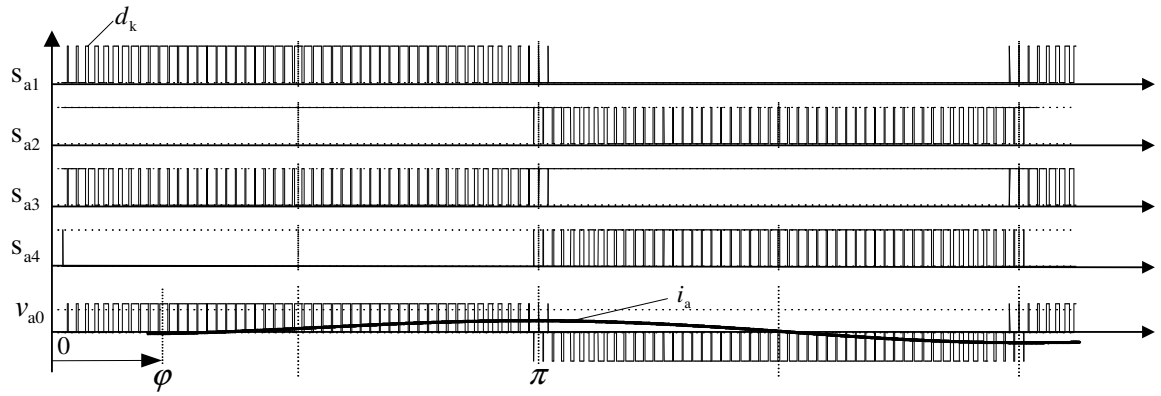

Fig.2. Gate signals and load current of phase A for three-level NPC inverter

The total power loss of the convert can be expressed as :

$$p_{inv} = 6\times(p_{conduct\text{-}half} + p_{sw\text{-}half}) \quad (1)$$

As apparent from Table1 and Fig.2, in (0~π) range of the reference voltage angle , S_{a1}, S_{a2}, S_{a3} and their corresponding anti-parallel diode and neutral point clamped diodes D_{5a}, D_{6a} , they both have conduction losses, the total conduction loss can be expressed as follows[8]-[10]:

$$p_{conduct\text{-}half} = p_{conduct\text{-}T} + p_{conduct\text{-}D} \quad (2)$$

$p_{conduct\text{-}T}$ and $p_{conduct\text{-}D}$ represent the main circuit switching loss and diode conduction loss, they can be expressed as follows :

$$\begin{aligned} p_{conduct\text{-}S} &= p_{conduct\text{-}Sa1} + p_{conduct\text{-}Sa2} + p_{conduct\text{-}Sa3} \\ p_{conduct\text{-}D} &= p_{conduct\text{-}Da1} + p_{conduct\text{-}Da2} + p_{conduct\text{-}Da5} + p_{conduct\text{-}Da6} \end{aligned} \tag{3}$$

Expand the formula (3):

$$P_{conduct\text{-}S} = \frac{T_s}{T} \cdot \sum_{k=k_\varphi}^{m_f/2-k_\varphi} v_{onSa1\_k} \cdot i_k \cdot d_k + \frac{1}{T}\left[\int_{t_{k\varphi}}^{T/2} v_{T0} + r_T \cdot i(t)\right] \cdot i(t)dt + \frac{T_s}{T} \cdot \sum_{k=1}^{k_\varphi} v_{onSa3\_k} \cdot i_k \cdot (1-d_k) \tag{4}$$

$$P_{conduct\text{-}D} = \frac{T_s}{T} \cdot \sum_{k=1}^{m_f/2} v_{onDa5\_k} \cdot i_k \cdot (1\text{-}d_k) + \frac{2T_s}{T} \cdot \sum_{k=1}^{k_\varphi} v_{onDa1\_k} \cdot i_k \cdot d_k \tag{5}$$

In the half period of the reference voltage command, switching loss of the power devices is as follows [10]-[12]:

$$p_{sw\text{-}half} = p_{sw\text{-}Sa1} + p_{sw\text{-}Sa3} + p_{rec\text{-}Da1} + p_{rec\text{-}Da2} + p_{rec\text{-}Da5} + p_{rec\text{-}Da6} \tag{6}$$

Expand the formula (6):

$$p_{sw\text{-}half} = \frac{1}{T} \cdot \sum_{k=k_\varphi}^{m_f/2-k_\varphi} (E_{swSa1\_k} + E_{recDa5\_k}) + \frac{1}{T} \cdot \sum_{k=1}^{k_\varphi} (E_{swSa3\_k} + E_{recDa6\_k} + E_{recDa1\_k} + E_{recDa2\_k}) \tag{7}$$

Power loss distribution simulation analysis were carried out on the 3L-NPC converter, the radio load current was set to 400A and the switching frequency was set to 1kHz, using SVPWM modulation algorithm and choosing the Infineon 650R17IE4 as the switching devices.

Fig.3 shows the simulation result of the power device dissipation in 3L-NPC converter, which in case of the inverter-mode and the rectifier-mode, modulation respectively 0.05 and 1.05. When the modulation index is 1.05 (Fig.3-b), S_{a1} occupy the maximum power loss, that is the outside device of the converter arm. In rectification mode, when modulation index is 0.05 (Fig.3-c), S_{a2} the inside device of the covert arm has the maximum power loss. Fig3-a and Fig3-b also appeared the similar power loss distribution by the analysis shows. It can be concluded that the topology of 3L-NPC converters have the disadvantage of unequal loss distribution in the same bridge arm, which will result in different power device junction temperature and will ultimately affect the maximum capacity of the converter.

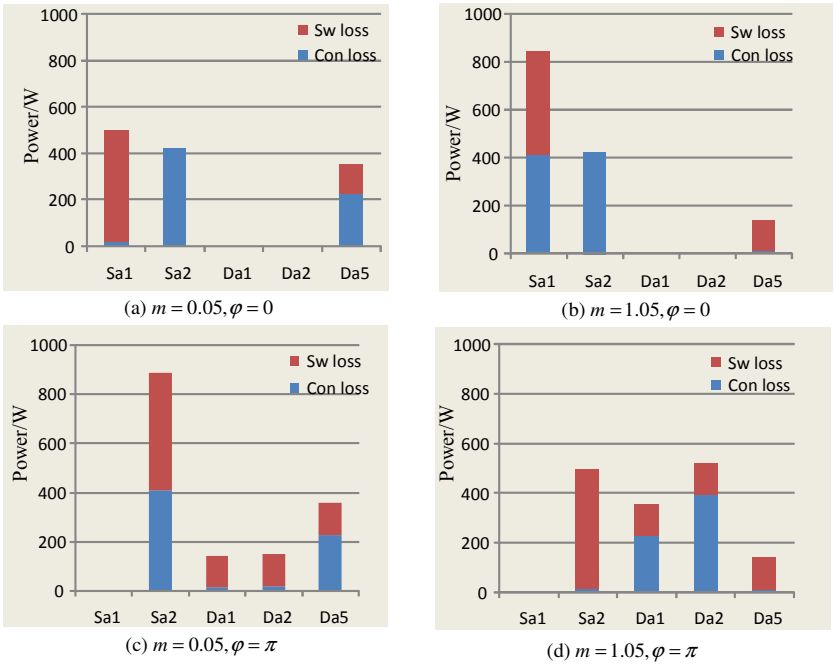

(a) $m=0.05, \varphi=0$ (b) $m=1.05, \varphi=0$

(c) $m=0.05, \varphi=\pi$ (d) $m=1.05, \varphi=\pi$

Fig.3. Distribution of Power losses In 3L-NPC with different work conditions

Table 3. Total losses distribution of 3L-NPC converter under different work conditions

Wok model	m=0.05	m=1.15
Inverter model (θ=0)	7689.6W	8440.2W
Rectifier model (θ=π)	9174W	9040.2W

4. Three level ANPC operating principle and power loss distribution

4.1 Three level ANPC operating principle analyze

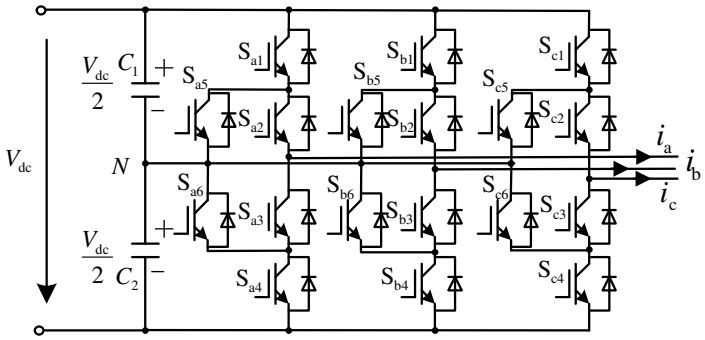

Fig.4. Topology of three-level ANPC converter

Three-level ANPC (3L-ANPC) structure using switching devices to replace the clamp diodes of three-level NPC topology, the structure is shown in Fig.4. Table 4 summarizes the switching states of 3L-ANPC topology , it has the same positive and negative switching states with 3L-NPC converter, in addition, it also has four additional zero states [10]-[12].

Table 4. Switch state s of the 3L-ANPC converter

Out Voltage v_{aN}	Switch States	Sa1	Sa2	Sa3	Sa4	Sa5	Sa6
V_{dc} / 2	P	1	1	0	0	0	1
0	0U2	0	1	0	0	1	0
0	0U1	0	1	0	1	1	0
0	0L1	1	0	1	0	0	1
0	0L2	0	0	1	0	0	1
$-V_{dc}$ / 2	N	0	0	1	1	1	0

The typical commutation path of 3L-ANPC is shown in Fig.5, combined with Table4, we can see that, no matter how the polarity of the load current, there are always two paths leading to the neutral point of the converter.

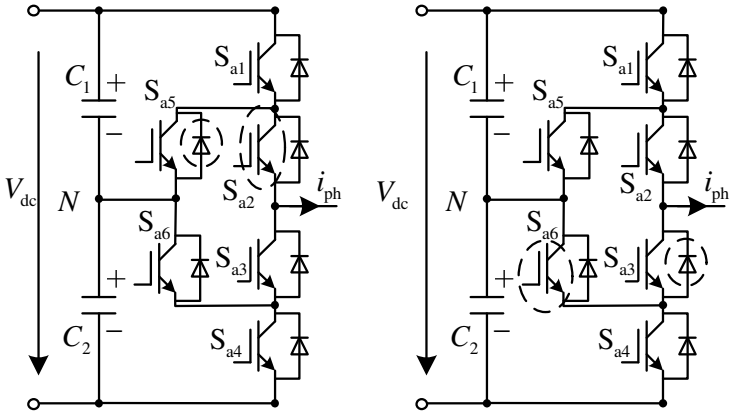

Fig.5. Commutation of three-level ANPC converter

In the 3L-ANPC topology, taking from the state "P" to the state "O" as an example, considering the 3L-ANPC converter output voltage and current are positive. when the converter output states change between P↔0U2, power loss focus on the outside of the bridge arm: switch S_{a1} and D_{a5}, when the converter output voltage states change between P↔0L1, power loss transfers to the inside of the bridge arm: switch S_{a2} and D_{a3}, therefore, if taken a reasonable control of the commutation order between P↔0U2 and P↔0L1, the unbalance power loss distribution in the same bridge arm of the 3L-NPC topology can be solved.

4.1 Three level ANPC power loss distribution analyse

Using the SPWM as the modulation algorithm of the 3L-ANPC, the principle of the algorithm is shown in Fig.6 [13]-[16].

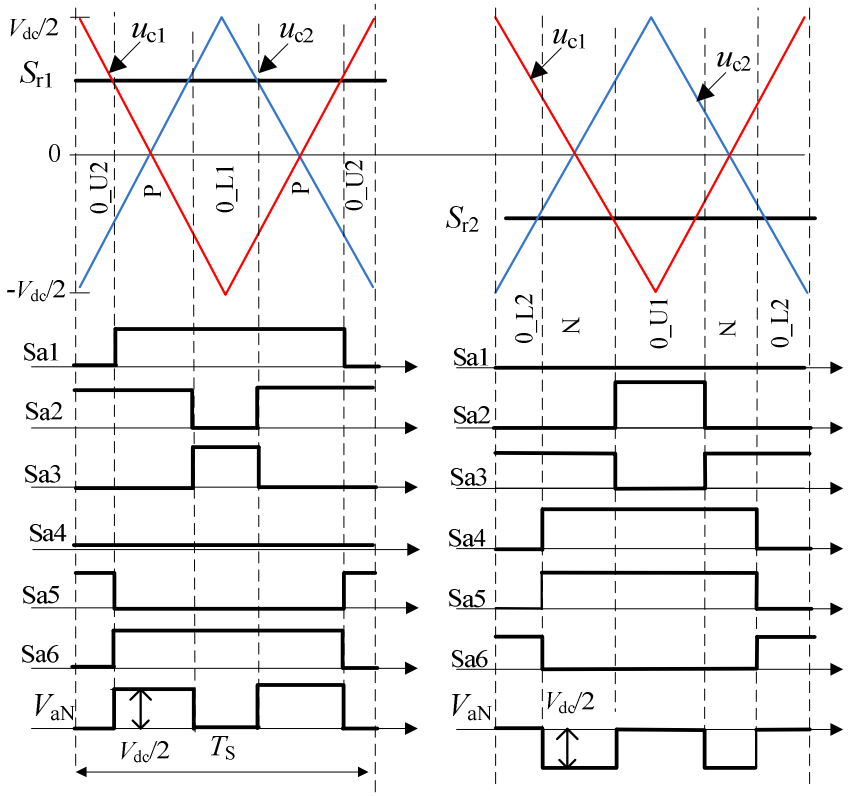

Fig.6. PWM strategy of three-level ANPC converter

In Fig.6 S_{r1} and S_{r2} are the reference voltage and U_{c1} and U_{c2} are the carrier signal, which are symmetrical on the horizontal coordinate, phase difference 180˚. When the voltage command is greater than zero, the comparison method is S_{r1} shown in Fig.6, in a switching cycle which includes 0U2, P, 0L1 three switching states, When the voltage command is less than zero, the comparison manner is S_{r2} shown in Fig.6, in a switching cycle which includes 0L2, N, 0U1 three switching states. As shown in Fig.6， the output frequency of the phase voltage V_{aN} is two times of the switching frequency of the power device, that the switching frequency has a feature of "natural doubling".

Formula (1) is still established for the total power loss of 3L-ANPC, assuming that the power factor angle is φ, in the (0~π) range of the reference voltage , the total conduction loss of the switching device of the inverter can be expressed as [10] [17][18]:

$$p_{conduct-S}=p_{conduct-Sa1}+p_{conduct-Sa2}+p_{conduct-Sa3}+p_{conduct-Sa5}+p_{conduct-Sa6} \tag{8}$$

Expand the formula (7):

$$P_{conduct-S}=\frac{T_s}{T}\cdot[\sum_{k=1}^{k_\varphi}(v_{onSa3,k}\cdot i_k\cdot G_{Sa3\bullet k}+v_{onSa5\bullet k}\cdot i_k\cdot G_{Sa5\bullet k})+\sum_{k=1}^{m_f/2}(v_{onSa1\bullet k}\cdot i_k\cdot d_k+ v_{onSa2\bullet k}\cdot i_k\cdot G_{Sa2\bullet k}+v_{onSa6\bullet k}\cdot i_k\cdot(1-d_k))] \tag{9}$$

The diode conduction loss can be expressed as follows :

$$p_{conduct-D}=p_{conduct-Da1}+p_{conduct-Da2}+p_{conduct-Da3}+p_{conduct-Da5}+p_{conduct-Da6} \tag{10}$$

Expand the formula (10):

$$P_{conduct-D}=\frac{T_s}{T}\cdot[\sum_{k=1}^{k_\varphi}(v_{onDa1\bullet k}\cdot i_k\cdot d_k+v_{onDa2\bullet k}\cdot i_k\cdot G_{Sa2\bullet k}+v_{onDa6\bullet k}\cdot i_k\cdot(1-G_{Sa2\bullet k}))+\sum_{k=1}^{m_f/2}(v_{onDa1\bullet k}\cdot i_k\cdot(1-d_k)+v_{onDa5\bullet k}\cdot i_k\cdot G_{Sa5\bullet k})] \tag{11}$$

The total switching loss of the inverter can be expressed as [16]-[18]:

$$p_{sw-half}=p_{sw-Sa1}+p_{sw-Sa2}+p_{sw-Sa3}+p_{sw-Sa5}+p_{rec-Da1}+p_{rec-Da2}+p_{rec-Da3}+p_{rec-Da5} \tag{12}$$

Expand the formula (12):

$$p_{sw-half}=\frac{1}{T}\cdot[\sum_{k=1}^{k_\varphi}(E_{swSa3\_k}+E_{recDa2\_k}+E_{swSa5\_k}+E_{recDa2\_k})+\sum_{k=1}^{m_f/2-k_\varphi}(E_{swSa1\_k}+E_{recDa3\_k}+E_{swSa2\_k}+E_{recDa5\_k})] \tag{13}$$

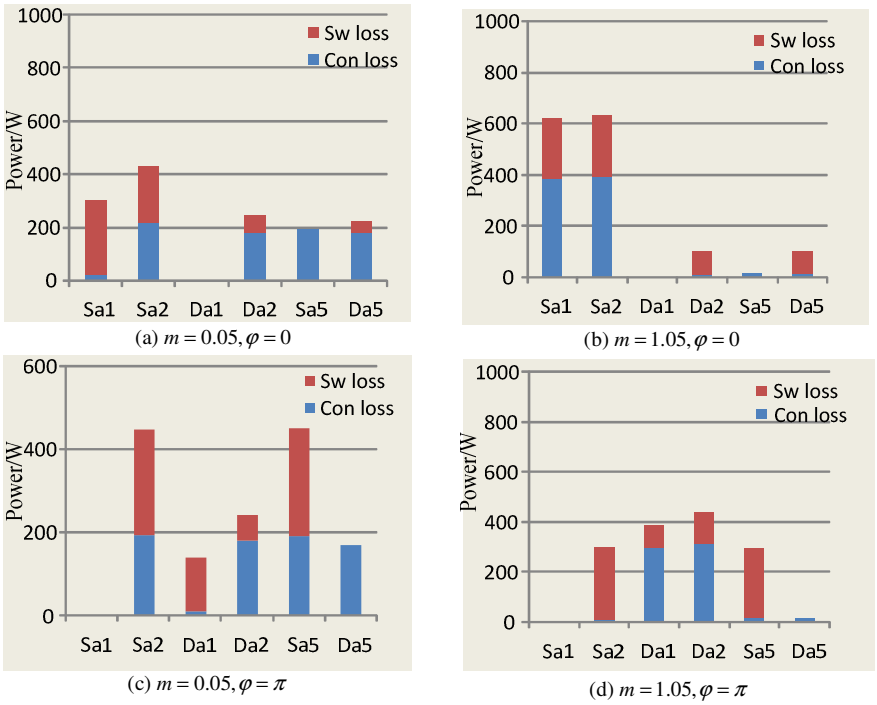

Fig.7. Distribution of Power losses In 3L-ANPC with different work conditions

Using the modulation strategy in Fig.6, the loss distribution of the 3L-ANPC has been carried out under difference work conditions, the simulation parameters and configuration are the same with the 3L-NPC described previous. Fig.7 shows the simulation result of the power device dissipation in 3L-ANPC converter, which in case of the inverter-mode and the rectifier- mode, with the modulation respectively 0.05 and 1.05. Compared with 3L-NPC, when the modulation index is 0.05and 1.05, in the same bridge arm, the switching loss distribution of the 3L-ANPC is more balance. Fig.8 shows the simulation results of the 3L-ANPC,its equal frequency is two times of 3L-NPC.

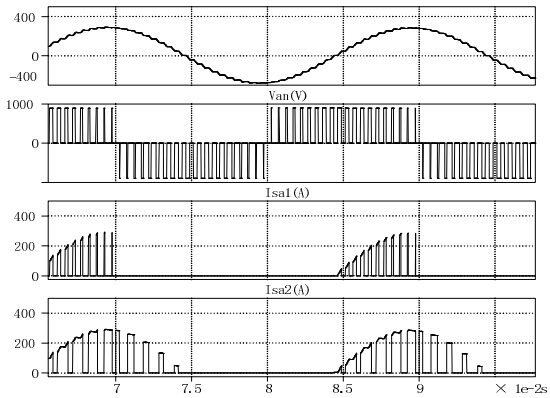

Fig.8. Simulation results of 3L-ANPC converter

Table 5 summarizes the total power loss of the 3L-ANPC under different wok conditions, compared with Table4, in the same woke condition, 3L-NPC and 3L-ANPC nearly have the same power loss, the advantage of 3L-ANPC lies in balancing the loss distribution of the power device in the same bridge arm.

Table 3. Total losses distribution of 3L-ANPC converter under different work conditions

Wok model	m=0.05	m=1.15
Inverter model (θ=0)	8210.4W	8817.2W
Rectifier model (θ=π)	8690W	8583.6W

5. Conclusion

This paper analysis the loss distribution model of 3L-NPC and 3L-ANPC respectively, the comparison results show that the 3L-NPC has the disadvantage of unequal loss distribution in the power devices of the same bridge arm. In contrast, the 3L-ANPC can achieve the distribution equal by switching different zero states. Using the SPWM as the modulation algorithm of 3L-ANPC. The simulation results show that, 3L-ANPC have the features of more balance power distribution and "natural doubling" switching frequency.

Acknowledgment

This work was supported by the National High Technology Research and Development Programme of China (863 Programme) under Grant No.2011AA050403.

References

[1] A. Nabae, I. Takahashi, and H. Akagi, A new neutral point clamped PWM inverter. *IEEE Trans on Industry Application,* 1A-17(5),518–523, 1981.

[2] Rodriguez. Jose, Bernet. Steffen, Steimer. Peter, K. Lizama, Ignacio E, A Survey on Neutral-Point-Clamped Inverters, *IEEE Trans on Industry Electrics,*57(1), 2219-2230.,2010.

[3] Clotea. L, Forcos. A, Marinescu. C, Georgescu. M. Power losses analysis of two-level and three-level neutral clamped inverters for a wind pump storage system, *Optimization of Electrical and Electronic Equipment (OPTIM)*, 1174-1179,2010.

[4] Andler, D., et al.. Experimental Investigation of the Commutations of a 3L-ANPC Phase Leg Using 4.5-kV - 5.5-kA IGCTs. *IEEE Transactions on Industrial Electronics*, 60(11): 4820-4830,2013.

[5] Andler, D., et al. Switching Loss Analysis of 4.5-kV-5.5-kA IGCTs Within a 3L-ANPC Phase Leg Prototype. *IEEE Transactions on Industry Applications*, 50(1): 584-592, 2014.

[6] Ke, M., et al,Thermal analysis of multilevel grid side converters for 10 MW wind turbines under Low Voltage Ride Through. *ECCE 2011*, 2117-2124, 2011.

[7] Long,C., et al.. Electro-thermal loss analysis of the 3L-ANPC converter. *2014 IEEE 5th International Symposium on Power Electronics for Distributed Generation Systems (PEDG)*, 1-5,2014.

[8] Senturk, O., et al, Power Capability Investigation Based on Electro-thermal Models of Press-pack IGBT Three-Level NPC and ANPC VSCs for Multi-MW Wind Turbines, *IEEE Transactions on Power Electronics*,

IPP(99): 1-1,2012.
[9] Senturk, O. S., et al, Converter Structure-Based Power Loss and Static Thermal Modeling of The Press-Pack IGBT Three-Level ANPC VSC Applied to Multi-MW Wind Turbines. *IEEE Transactions on Industry Applications*,47(6),2505-2515, 2011.
[10] Barater, D., et al. Performance evaluation of a 3-level ANPC photovoltaic grid-connected inverter with 650V SiC devices and optimized PWM. *Energy Conversion Congress and Exposition (ECCE*2014),2233-2240, 2014.
[11] Andler. D, Hauk. E, Alvarez. R, Weber. J, Bernet. S, Rodriguez. J. New junction temperature balancing method for a three level active NPC converter, *(EPE 2011)*,1-9, 2011.
[12] Kui, W., et al. Neutral-point potential balancing control of three-level ANPC converters based on zero-sequence voltage injection using PS-PWM. *2013 International Conference on Electrical Machines and Systems (ICEMS)*,1688-1692,2013.
[13] Floricau. D, Floricau. E, Gateau. G. Three-level active NPC converter: PWM strategies and loss distribution, *IECON 2008*,3333-3338, 2008.
[14] Fazio, P., et al. Fault detection and reconfiguration strategy for ANPC converters. *Power Electronics and Motion Control Conference* 2012 ,DS1b.17.1-5,2012.
[15] Gurpinar, E., etal. Performance analysis of SiC MOSFET based 3-level ANPC grid-connected inverter with novel modulation scheme. *IEEE 15th Workshop on Control and Modeling for Power Electronics (COMPEL)*, 1-7,2014.
[16] Jun, L., et al.Reliability comparison for 3L-NPC and 3L-ANPC converters for drives application. *2011 IEEE International Electric Machines & Drives Conference (IEMDC)*, 271-276, 2011.
[17] Bruckner. T, Bernet. S, Guldner. H. The active NPC converter and its loss-balancing control. *IEEE Trans on Industry Electrics*,52(3), 855-868, 2005.
[18] Andler, D., et al. Improved model predictive control with loss energy awareness of a 3L-ANPC voltage source converter. *2010 International Conference on Applied Electronics (AE)*, 1-6,2010.